

Experimental Observation of Critical Phenomena in a Laser Light System

Amir Rosen, Rafi Weill, Boris Levit, Vladimir Smulakovsky, Alexander Bekker, and Baruch Fischer

Department of Electrical Engineering, Technion, Haifa 32000, Israel

(Received 26 April 2010; published 2 July 2010)

We experimentally demonstrate critical behavior of a passively mode-locked laser with properties that are similar to those of gas-liquid and magnetic spin systems. The laser light modes provide a special nonthermodynamic many-body system where noise takes the role of temperature. It is also a rare opportunity of an experimental pure one-dimensional system. As theoretically predicted, we identified in the laser light-mode system two thermodynamiclike phases, one characterized by *spontaneous pulses* and the second by field-induced *parapulses*, separated by a first order phase transition boundary that is terminated by the critical point. We also measured the critical exponents, $\beta \approx 0.52$, $\gamma \approx 1$, and $\delta \approx 3.1$, which are close to the mean field values that are exact in the laser system.

DOI: 10.1103/PhysRevLett.105.013905

PACS numbers: 42.55.Ah, 05.70.Fh, 42.65.-k

Phase transitions and critical phenomena are manifestations of dramatic changes and discontinuities of macroscopic properties in systems with a large number of interacting degrees of freedom [1,2]. While those ideas reached and influenced very different fields like biology [3] and economy [4], experimental observations in physics have been mostly concentrated in material systems, atomic or molecular. Canonical examples are the gas-liquid-solid and magnetic spin systems. This work deals with a non-thermodynamic many-body laser light system.

Lasers that support a large number of axial modes, such that are needed, for example, in mode locking for producing ultrashort light pulses [5,6], were shown to follow strict statistical mechanics rules given by the statistical light-mode dynamics (SLD) theory [7–13] where noise takes the role of temperature. The situation is very similar to the classical examples of magnetic spin and gas-liquid-solid systems. It was theoretically and experimentally shown that pulse formation in passive mode locking is a first order phase transition where the light-mode system becomes ordered [7,8,12]. The varied parameters were power and/or noise (“temperature”) that were controlled by the amount of pumping and/or injection into the cavity of outside noise (that adds to the basic quantum noise). A more recent finding was the prediction [14] and the experimental demonstration of Bose-Einstein condensation in active mode-locked lasers.

It was theoretically shown that passively mode locked (PML) lasers can exhibit critical behavior when external light pulses are injected into the laser cavity [11]. The injected light takes the role of pressure in gas-liquid-solid systems or the external magnetic field in spin systems. The many light-mode system tends to produce pulses due to the mode aligning force of the saturable-absorber nonlinearity, but at nonzero noise (“temperature”) levels the entropy pushes the mode system (the phases) to randomness and a quasi continuous wave (CW) operation. The injection joins forces with the saturable-absorber for aligning the mode phasors, promoting pulse operation. Therefore, just as spin

systems can have spontaneous magnetization, paramagnetization when an external magnetic field induces spin orientation (para-magnet), and no-magnetism (spin disorder), we can have in the PML laser spontaneous-pulse, parapulse, and no-pulse regimes.

The SLD theory for the complex many mode PML laser system with externally injected pulses can be summarized by one very simple equation from which we can derive the system properties. It is the thermodynamiclike potential obtained in Ref. [11] [Eq. (10) with $n = 1$]:

$$f = -\frac{\gamma_s}{2}x^4 - T \log(P - x^2) - 2hx, \quad (1)$$

where x is the light pulse amplitude, P is the total laser cavity power, T is the noise strength, that takes the role of temperature, h is the light pulse injection amplitude (“external field”), and γ_s is the nonlinear saturable-absorber coefficient [5,7]. The normalized pulse amplitude $\tilde{x} = x/P^{1/2}$ (therefore, $\tilde{x} \in [0, 1]$) can be viewed as an order parameter of the mode system, analogously to the density in gas-liquid solids and the magnetization in magnetic spin systems. In reduced variables, $\tilde{x} = x/P^{1/2}$, $\tilde{T} = T/(\gamma_s P^2)$, and $\tilde{h} = 2h/(\gamma_s P^{3/2})$, Eq. (1) can be written as $\tilde{f} = -(\tilde{x}^4/2) - \tilde{T} \log(1 - \tilde{x}^2) - \tilde{h} \tilde{x}$, up to unimportant additive terms independent of x (or m) and γ_s . The analysis that leads to f in Eq. (1) can be done in the spatial or the frequency domain [11]. The injected pulse train with a rate that matches the laser cavity roundtrip can be viewed in the frequency domain by a phase aligned frequency comb that by proper synchronization overlap the laser axial modes. It therefore acts on the laser modes’ phases as an aligning force, in a similar way that an applied magnetic field induces alignment in a spin system. We add that f in Eq. (1) relates to the simple case of one pulse in the cavity [8,11]. We also stress that Eq. (1) was obtained in the mean field theory that in our case was shown to be exact in the thermodynamics limit of a large number of modes. Therefore, the results derived from f , including the critical exponents, are exact. The PML laser system is therefore a

special statistical mechanics example where the classical mean field formalism is exact.

f consists of three terms: The first is the “internal energy” from the nonlinear mode interaction due to the saturable absorber, that works for mode ordering and short pulses. The second term is the opposite force of entropy that makes its living from the many disordered configurations. This is the important addition of the SLD theory. The last term is the external field by the external pulse train that works for the alignment of the modes and pulse formation. It is then the combination of all these parts that gives the free energy and the laser system behavior.

The properties of the PML laser system can be derived from the thermodynamiclike potential f . The x that gives the global minimum of f , determines the expectation value of the pulse amplitude $m = \langle x \rangle$, which can be viewed as an order parameter in our laser system. Calculating $\tilde{m} = m/P^{1/2}$ as a function of $\tilde{T} = T/(\gamma_s P^2)$ and \tilde{h} yields the phase diagram shown in Fig. 1, with two phases: In one, the pulse is induced by the injection and therefore we call it the parapulse phase. It includes a no-pulse case for zero external field⁶, at the $\tilde{h} = 0$ line for $\tilde{T} > 0.2036$. The second phase is characterized by a strong spontaneous pulse (forced by the saturable-absorber nonlinearity). The phases are separated by a first-order phase transition line, the coexistence curve, characterized by an abrupt change of the pulse amplitude. The discontinuity becomes smaller until it vanishes at the critical point: $(\tilde{T}_C, \tilde{h}_C, \tilde{m}_C) \approx (0.34, 0.20, 0.53)$. For obtaining the critical exponents, we applied a small deviation analysis of the minimum of the free energy near the critical point [11]. The critical expo-

nents are given by $(m_C - m) \propto (T_C - T)^\beta$ when the critical point is approached along the coexistence curve, $(m_C - m) \propto |h_C - h|^{1/\delta}$ for approaching along the h axis or along any other than the coexistence curve direction in the P - h plane, and $\partial(m_C - m)/\partial h \propto (T_C - T)^{-\gamma}$ along the coexistence curve. The predicted exponents in our system are [11] $\beta = 1/2$, $\gamma = 1$, and $\delta = 3$. These are the mean-field values which are exact in our system.

The experimental setup we used to verify the theory, schematically shown in Fig. 2, consisted of an erbium-doped fiber ring laser, ≈ 20.7 m long, corresponding to 10 MHz cavity resonance. It is a single (lateral) mode fiber, and therefore the laser system is one-dimensional. The saturable absorber was provided by the nonlinear polarization rotation effect in the fiber combined with polarizers in the cavity. Matching the external pulse rate and its synchronization to the spontaneous pulse was a major challenge in the experiment. We solved that by deriving the external pulse train from the mode-locked laser itself that was operated such that it already generated one pulse. We then amplified the pulse train outside the laser, filtered it, temporally, to eliminate noise from out of the pulse region, and spectrally, capturing the spectral region of a Kelly sideband [15], having a soliton spectrum, and differentiating it from the unfiltered pulse. Then after controlling its strength by a variable attenuator, the external pulse was injected into the laser at a far site from the first pulse in the cavity, where we followed a new pulse formation. This new pulse was the target of our measurements. The first pulse with a constant power that reached the saturation value [8] with its negligible entropy could be omitted from the

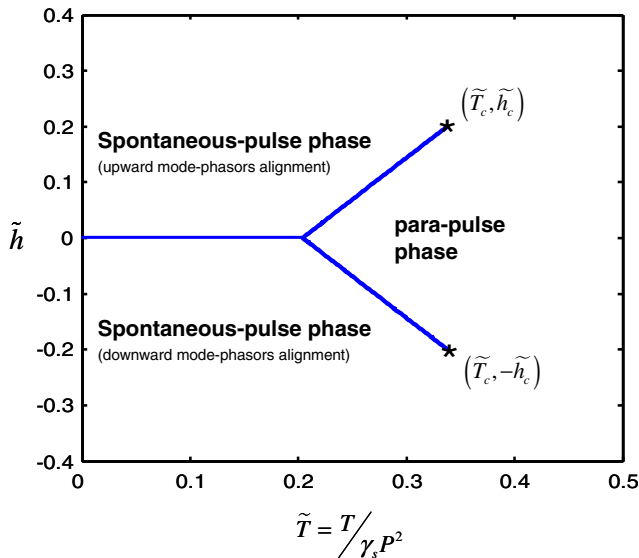


FIG. 1 (color online). Theoretical phase diagram in the \tilde{T} - \tilde{h} plane of the PML laser with external pulse injection: The lines are the boundary with first order phase transition between the parapulse and spontaneous-pulse phases, terminated at the critical point $(\tilde{T}_C, \tilde{h}_C)$, where the phase transition discontinuity disappears.

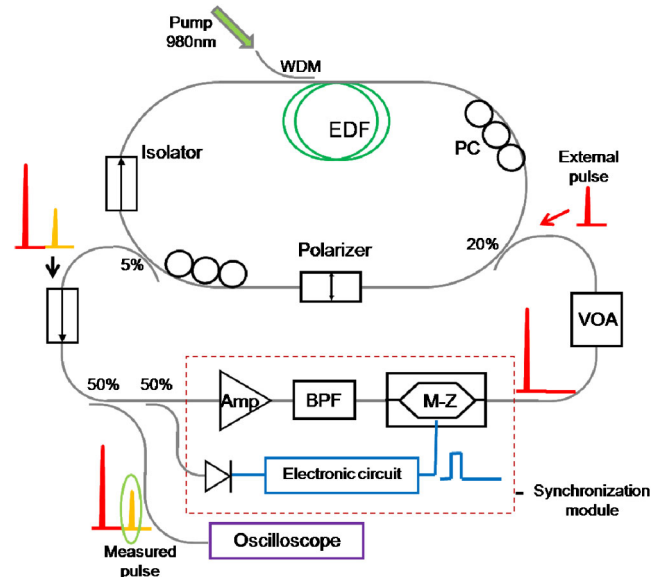


FIG. 2 (color online). Experimental setup of the actively mode-locked fiber laser with an external pulse source: erbium-doped fiber (EDF), polarization controller (PC), wavelength division multiplexer coupler (WDM), variable optical attenuator (VOA), Mach-Zehnder modulator (M-Z), band-pass filter (BPF), optical amplifier (Amp).

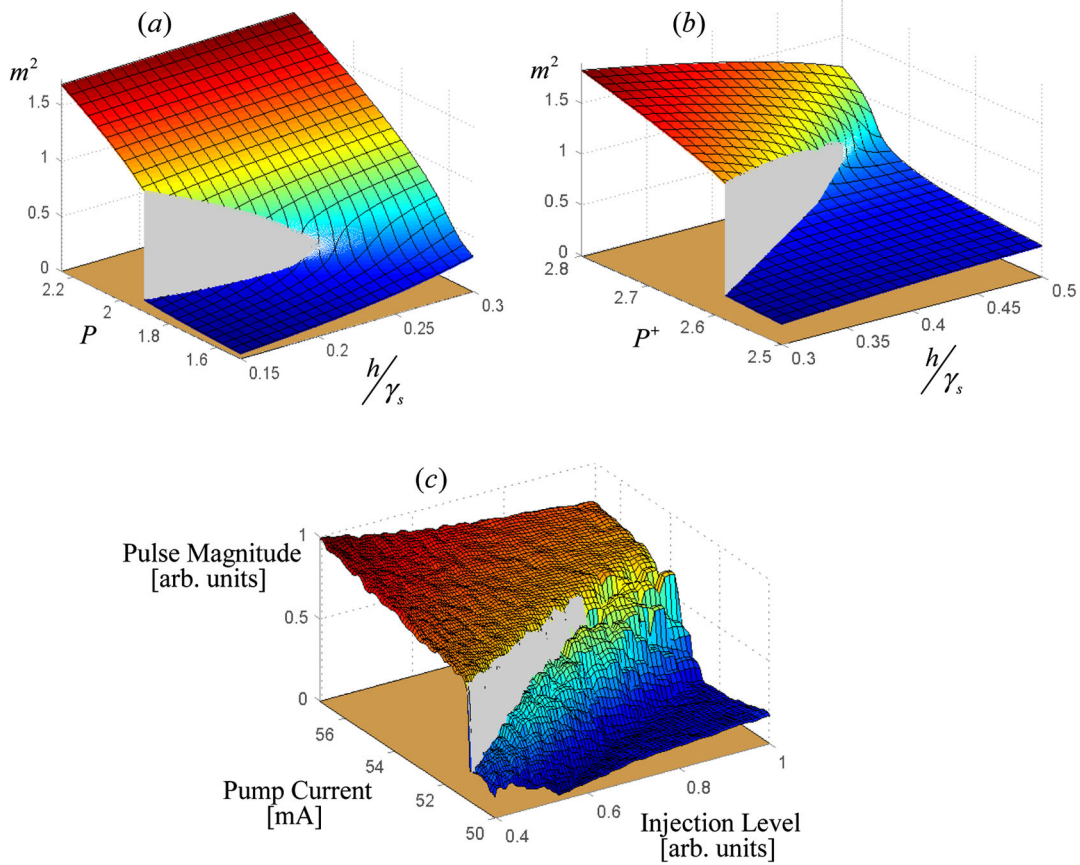


FIG. 3 (color online). Pulse power as a function of P and h : (a) Theoretical graph. (b) Theoretical graph with added noise from the external pulse injection, $T = T_0 + ah$, (with $T_0 = 1$ and $a = 3.3$) that renormalizes P that is then denoted by P^+ . (c) Experimental graph that is similar to the theoretical prediction in (b). We can see in the figures the para- and spontaneous-pulse regimes separated by a first-order phase transition discontinuity which narrows to zero at the critical point. Beyond this point there is a continuous transition between the two phases. For large P and h we see in the experimental graph the pulse saturation effect [9]. The experimental pulse power waveforms along two paths in the phase diagram are shown in Movie 1 of the supplementary material [16].

calculations and therefore did not affect the new pulse formation. For the new pulse, at its formation stage it is below the saturation regime [8]. However, as P and h increase we can observe in the experiment [Fig. 3(c)] the saturation effect, that can be accounted for by higher order nonlinear saturation terms [9]. The total power in the cavity was varied by changing the pumping of the laser amplifier. The data were taken from a small portion of the laser light that was coupled out to the measuring equipment. In the measurement process we scanned the P - h plane in the area shown in Fig. 3(c), varying P for a specific h , obtaining a matrix of 71×81 measurement points. We also note that the scanning direction was from the parapulse to the spontaneous-pulse phase, and we were careful in avoiding hysteresis effects [10].

Figure 3 and Movie 1 of the supplementary material [16] show the measurement results on the dependence of the pulse power as a function of P and h . It is a measure of the pulse energy since the pulse width in the experiments of ≈ 1 psec was significantly shorter than the measurement resolution that was ≈ 10 psec. P was varied by changing the current injection to the pump laser diode, but since the

relevant variable is $\tilde{T} = T/(\gamma_s P^2)$ we could vary T , instead of P , by changing the external noise injection level and keeping P constant [8,12]. h was varied by controlling the external injection strength. We have found that the external pulse injection, although filtered, added noise to the cavity and thus changed T as well. This factor was taken into account in the data analysis by adding it to the laser noise T_0 , so that $T = T_0 + ah$. Figure 3(b) shows the theoretical diagram that includes the additional noise, with $T_0 = 1$ and $a = 3.3$ that were found to fit the experimental measurements, shown in Fig. 3(c).

The graphs show the abrupt first-order phase transition as $P \propto 1/\tilde{T}$ is varied. As h and P increase, the line that follows the discontinuity in m draws the boundary (coexistence line) between the parapulse and the spontaneous-pulse phases. The discontinuity narrows to zero at the critical point, and beyond it m changes continuously. This measured phase diagram is remarkably similar to the theoretical prediction shown in Fig. 3(b).

We now turn to the measurements that provide the critical exponents in our experimental system. Figure 4 shows graphs of $(m_c^2 - m^2)$ near the critical point along

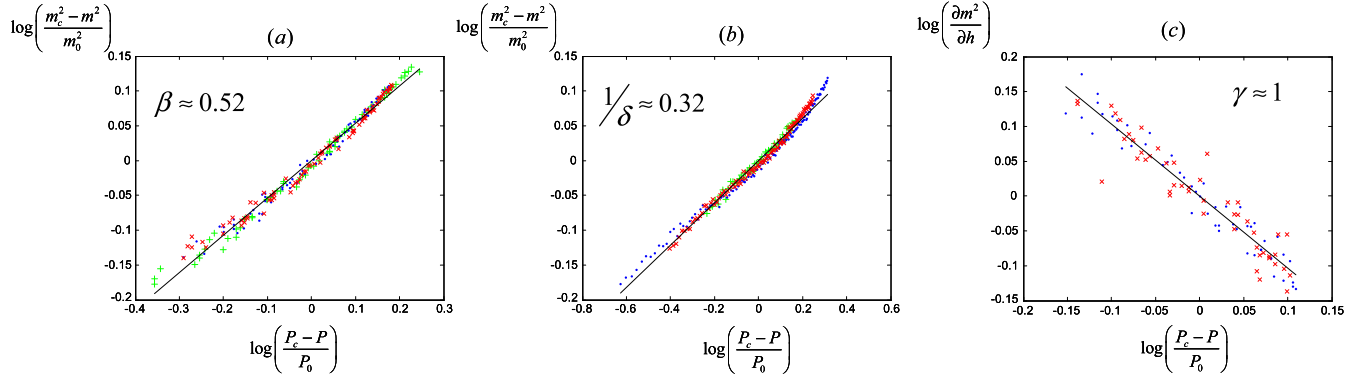


FIG. 4 (color online). Measurements near the critical point, obtaining the three critical exponents β , γ , and δ : Since we are interested in the graphs slope in log-log scales, we used dimensionless variables, normalized by arbitrary constants to move the curves center close to the axes origin. The data was taken from a few measurement sets, shown in different dot shapes and colors. (a) For β : Plot of $\log[(m_c^2 - m^2)/m_{\text{arb}}^2]$ as a function of $\log[(P - P_C)/P_{\text{arb}}]$, where the critical point is approached along the coexistence curve. Since near the critical point $(m_c^2 - m^2) \approx 2m_C(m_C - m)$, the slope of the linear fit gives the exponent $\beta = 0.52$. The theoretical value is $\beta = 1/2$. (b) For δ : Plot of $\log[(m_c^2 - m^2)/m_{\text{arb}}^2]$ as a function of $\log[(P - P_C)/P_{\text{arb}}]$ where the critical point is approached along the P axis. The slope of the linear fit gives the exponent: $1/\delta = 0.32$. The theoretical value is $1/\delta = 1/3$. (c) For γ : Plot of $\log[\frac{\partial}{\partial h}(m_c^2 - m^2)/m_{\text{arb}}^2]$ as a function of $\log[(P - P_C)/P_{\text{arb}}]$ where the critical point is approached along the coexistence curve. The derivative procedure results more scattered data points compared to the two former figures. The slope of the linear fit gives the exponent $-\gamma \approx -1$. The theoretical value is $\gamma = 1$.

two different directions in the (P, \tilde{h}) plane. Figure 4(a) it is along the coexistence curve and Fig. 4(b) is along P , changing P and keeping $h = h_c$ constant. In Fig. 4(c) it is again along the coexistence curve. We note about the axes in the graphs that the dependence is on $(P_C - P)$ (in log-log scales) that gives the same results as plotting against $(T_C - T)$. In addition, the measurements in the graph were of the pulse power, but we obtain from them the right exponents, since $(m_c^2 - m^2) \approx 2m_C(m_C - m)$. A linear fit was added to each of the plots. The slopes give the experimental critical exponents, found to be $\beta \approx 0.52$, $\delta \approx 3.1$, and $\gamma \approx 1$, very close to the theoretical values, $\beta = 1/2$ and $\delta = 3$, and $\gamma = 1$. We thus experimentally verified the exact SLD mean field theory in the PML laser system [11].

Conclusion.—We have experimentally shown critical behavior of light in a passively mode-locked laser with properties that are very similar to those of classical thermodynamic systems. We have measured and shown the system phase diagram and the critical exponents that follow and match the exact mean field theory. The laser light system provides a special nonthermodynamic one-dimensional many body system that deepens the understanding of mode locking and provides a new experimental statistical mechanics example.

This research was supported by the Israel Science Foundation.

*fischer@ee.technion.ac.il

[1] H. E. Stanley, *Introduction to Phase Transitions and Critical Phenomena* (Oxford University Press, N.Y., Oxford, 1971).

- [2] I. D. Lawrie and S. Sarbach, *Phase Transition and Critical Phenomena*, edited by C. Domb, and J. L. Lebowitz (Academic, London, 1984), Vol. 9.
- [3] S. V. Buldyrev, N. V. Dokholyan, A. L. Goldberger, S. Havlin, C. K. Peng, H. E. Stanley, and G. M. Viswanathan, *Physica (Amsterdam)* **249A**, 430 (1998).
- [4] T. Lux and M. Marchesi, *Nature (London)* **397**, 498 (1999).
- [5] H. A. Haus, *IEEE J. Sel. Top. Quantum Electron.* **6**, 1173 (2000).
- [6] T. R. Schibli, O. Kuzucu, J-W. Kim, E. P. Ippen, J. G. Fujimoto, F. X. Kaertner, V. Scheuer, and G. Angelow, *IEEE J. Sel. Top. Quantum Electron.* **9**, 990 (2003).
- [7] A. Gordon and B. Fischer, *Phys. Rev. Lett.* **89**, 103901 (2002).
- [8] B. Vodonos, R. Weill, A. Gordon, V. Smulakovsky, A. Bekker, O. Gat, and B. Fischer, *Phys. Rev. Lett.* **93**, 153901 (2004).
- [9] M. Katz, A. Gordon, O. Gat, and B. Fischer, *Phys. Rev. Lett.* **97**, 113902 (2006).
- [10] O. Gat, A. Gordon, and B. Fischer, *Phys. Rev. E* **70**, 046108 (2004); *New J. Phys.* **7**, 151 (2005).
- [11] R. Weill, A. Rosen, A. Gordon, O. Gat, and B. Fischer, *Phys. Rev. Lett.* **95**, 013903 (2005).
- [12] A. Gordon, B. Vodonos, V. Smulakovsky, and B. Fischer, *Opt. Express* **11**, 3418 (2003).
- [13] R. Weill, B. Vodonos, A. Gordon, O. Gat, and B. Fischer, *Phys. Rev. E* **76**, 031112 (2007).
- [14] R. Weill, B. Fischer, and O. Gat, *Phys. Rev. Lett.* **104**, 173901 (2010).
- [15] S. M. Kelly, *Electron. Lett.* **28**, 806 (1992).
- [16] See supplementary material at <http://link.aps.org/supplemental/10.1103/PhysRevLett.105.013905>.